Dihydrogen bond cooperativity in $(HCCBeH)_n$ clusters

Ibon Alkorta,[1,a] José Elguero,[1] and Mohammad Solimannejad[2]
[1]*Instituto de Química Médica (CSIC), Juan de la Cierva, 3, E-28006 Madrid, Spain*
[2]*Quantum Chemistry Group, Department of Chemistry, Arak University, 38156-879 Arak, Iran*

(Received 14 August 2007; accepted 9 July 2008; published online 14 August 2008)

A theoretical study has been carried out on the clusters formed by the association of ethynylhydroberyllium (HC≡CBeH) monomers. The monomer presents a linear disposition with a dipole moment of 0.94 D. Clusters from two to six monomers have been calculated for three different configurations (linear, cyclic with dihydrogen bonds, and cyclic with hydrogen bonds to the π-cloud), the third one being the most stable. The electronic properties of the clusters have been analyzed by means of the atoms in molecules and natural bond orbitals methodologies. Cooperative effects, similar to the ones described for standard hydrogen bonded clusters, are observed in those configurations where dihydrogen bonds are the main interacting force. © *2008 American Institute of Physics*. [DOI: 10.1063/1.2966007]

I. INTRODUCTION

Hydrogen bond (HB) formation induces changes within the monomers that are involved in it. In many cases, these changes facilitate the aggregation of additional monomers to the initially formed complex. This phenomenon is known as cooperativity or nonpairwise effect. It greatly influences the properties of the monomers and those of the formed clusters. Thus, for instance, the water trimer shows a basicity comparable to that of ammonia.[1–3] A number of theoretical studies have been devoted to analyze the cooperativity effects in hydrogen bonded systems.[4]

One of the most recent incorporations to the field of HBs corresponds to those cases where the HB acceptor is a negatively charged hydrogen. These interactions have been named dihydrogen bonds (DHBs). They were first reported in 1968,[5] then developed by Crabtree *et al.*,[6] and reviewed several times.[6–9] The DHB characteristics from a theoretical point of view were described by Popelier[10] in 1998, by Grabowski *et al.* in 2004 (Ref. 11) and 2007 (Ref. 12), and by some of us in 1996 (Ref. 13) and 2006.[14] DHB is in general a dead-end interaction while in standard HB, the same group that acts as HB donor can act simultaneously as HB acceptor (the HB network in the different structures of ice and water are a clear example of this fact). A few studies have reported the cooperativity in systems where one of the interactions corresponds to DHB.[15,16] Thus, to the best of our knowledge, no previous study has addressed the cooperativity in DHBs alone.

Some molecules are able to form long linear chains called catemers through the use of HBs [Scheme 1(a)], a typical example being HCN.[17–19] There are very few other possibilities. One of them, based on DHBs, is schematized in Scheme 1(b).The system chosen in the present article, HC≡CBeH, has the HB donor and acceptor groups in both extremes of the molecule and based on these characteristics can be considered an analog of HCN and HNC. The hydrogen bonded clusters of HCN can be obtained in linear or cyclic dispositions and have shown to present cooperativity effects that have been characterized experimentally and theoretically.[4,18–20] The HCCBeH molecule has been experimentally described in the laser ablation of acetylene with beryllium and characterized based on the IR spectra and density functional theory (DFT) calculations [B3LYP/6-311G(*d*)].[21]

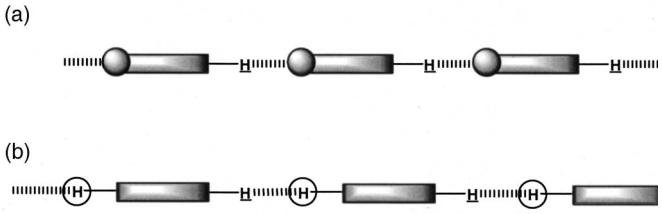

SCHEME 1. Underlined: acid atom; encircled: basic moieties.

II. METHODS

The geometry of the systems has been optimized in linear and cyclic configurations with $C_{\infty v}$ and D_{nh} symmetries, respectively. *Ab initio* calculations have been carried out with the GAUSSIAN-03 package.[22] The computational level chosen include the B3LYP/6-31+G(*d*,*p*),[23–25] M05/6-31+G(*d*,*p*),[26] MP2/6-31+G(*d*,*p*), MP2/6-311++G(2*d*,2*p*), and MP2/aug-cc-pVTZ ones.[27–29] In addition, single point calculations have been carried out at the CCSD(T)/aug-cc-pVTZ//MP2/aug-cc-pVTZ computational level. Frequency calculations have been carried out on the optimized geometries obtained at B3LYP/6-31+G(*d*,*p*), M05/6-31+G(*d*,*p*), and MP2/6-31+G(*d*,*p*) at the same computational level. The DFT calculations have been carried using the ultrafine option for the integrals.

Ab initio supermolecule calculations are known to be susceptible to basis set superposition error (BSSE) when

[a]Author to whom correspondence should be addressed. Electronic mail: ibon@iqm.csic.es. FAX: 34-91-564-48-53.

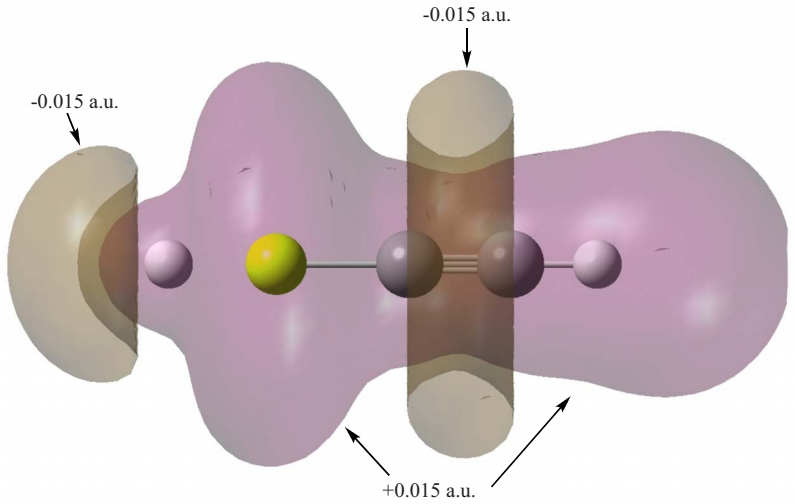

FIG. 1. (Color online) MEP of HCCBeH. The values of the isosurfaces shown are ±0.015 a.u. (pink: positive; gray: negative).

finite basis sets are used. The most common way to correct the BSSE is with the full counterpoise method.[30] Systematic studies at the restricted Hartree Fock (RHF) level have indicated that the counterpoise corrected interaction energies are no more reliable than the uncorrected ones.[31] At correlated levels, the application of the full counterpoise method caused a nonphysical increase in the dimension of *virtual space*.[32] Since the inclusion of diffuse functions has been shown to markedly reduce the BSSE effect,[33,34] the interaction energy of the clusters in the present article has been calculated as the difference between the supermolecule and the sum of the isolated monomers in their minimum configuration.

The electron density obtained at the MP2/6-31 +G(d,p) computational level has been analyzed based on the atoms in molecules (AIM) methodology[35] with the AIMPAC,[36] MORPHY98,[37] and AIM2000 programs.[38] The atomic integrations have been carried out to obtain small values of the integrated Laplacian for all the atoms. Ideally, a perfect integration within an atomic basin should provide a null integrated Laplacian. We have shown that values of the integrated values smaller than 1×10^{-3} for all the atoms of a given system provide small energetic and charge errors when the sum of the atomic contributions are compared to those obtained with the *ab initio* methods for the whole system.[39]

The natural bond orbitals (NBOs) method[40] has been used to analyze the intermolecular interaction between occupied and empty orbitals. These interactions are of main importance in the formation of hydrogen bonded clusters.

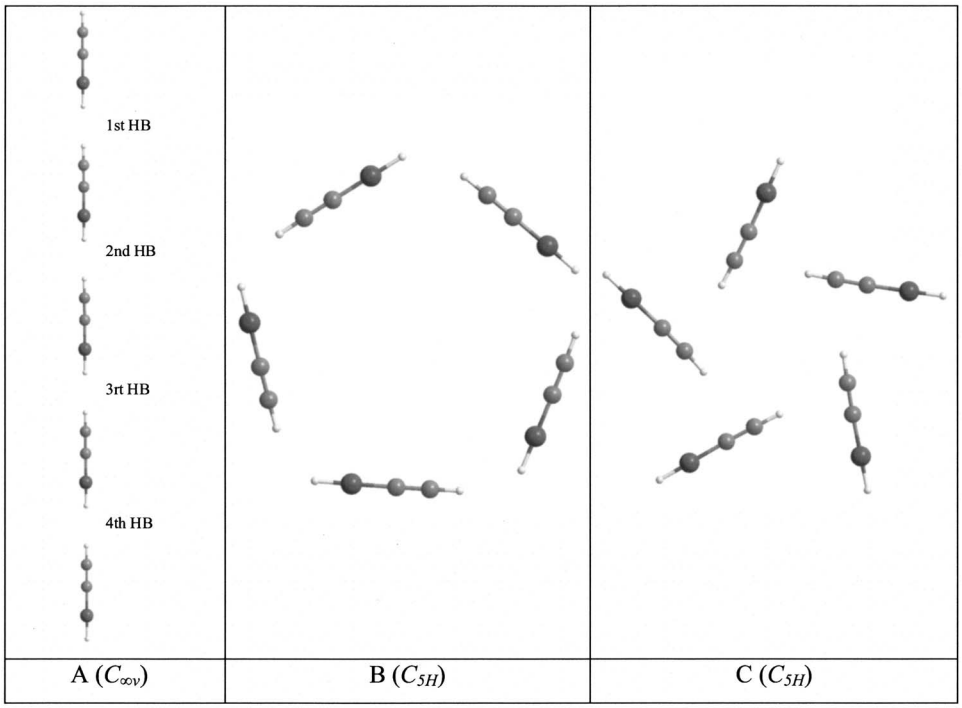

FIG. 2. Example of the three configurations considered for the pentamer. The symmetry of each cluster is shown.

TABLE I. Total interaction energy (kJ/mol) of the complexes studied.

Config. (no. of monomers)	B3LYP/6-31+G (d,p)	M05/6-31+G (d,p)	MP2/6-31+G (d,p)	MP2/6-311++G $(2d,2p)$	MP2/aug-cc-pVDZ	MP2/aug-cc-pVTZ	CCSD(T)/aug-cc-pVDZ
A (2)	−4.29	−5.54	−5.29	−5.87	−8.13	−6.88	−8.02
A (3)	−8.80	−11.29	−10.80	−11.94	−16.78	−13.88	−16.56
A (4)	−13.36	−17.09	−16.35	−18.02	−25.44		−25.11
A (5)	−17.94	−22.90	−21.93	−23.97			
A (6)	−22.54	−28.71	−27.51				
B (3)	−7.54	−16.02	−16.65	−18.91	−21.48	−21.05	−20.71
B (4)	−12.05	−19.16	−18.75	−20.22	−26.14		−25.16
B (5)	−17.85	−25.42	−24.61	−25.88			
B (6)	−23.36	−31.80	−30.63				
C (2)	−3.81	−6.86	−9.97	−8.51	−11.20	−9.74	−10.53
C (3)	−10.66	−19.45	−27.41	−23.95	−31.56	−27.22	−29.21
C (4)	−17.63	−29.91	−44.61	−37.29	−49.07		−45.84
C (5)	−21.15	−37.85	−55.03	−47.18			
C (6)	−23.70	−45.53	−63.15				

III. RESULTS AND DISCUSSION

A. Monomers

The H−C≡C−Be−H molecule presents a linear disposition with a small calculated dipole moment, 0.94 D at the MP2/6-31+G(d,p) computational level. The molecular electrostatic potential (MEP) of this molecule presents a negative region in the axis close to the hydrogen atom attached to Be and a positive one in the opposite extreme of the molecule (see Fig. 1). These two groups can act as HB acceptor and donor, respectively. In addition, a torus shape region around the triple bond with negative values of the MEP is observed.

B. Clusters: Energy and geometry

Three different configurations have been considered for the clusters of the HCCBeH systems: (i) a linear one with DHB interactions (A), (ii) a cyclic one through DHB interactions (B), and (iii) a cyclic one where the HBs are between the π-cloud of the triple bond and the protic hydrogen of another molecule (C) (see Fig. 2 for an example). The calculated interaction energies of these clusters are gathered in Table I. The results show clearly the poor behavior of the B3LYP functional in the description of the interaction energies probably due to the bad description of the dispersion forces that should be very important in these weak complexes. Thus, the B3LYP calculations can only be used as a good geometrical starting point for higher calculations in the present case. The M05 results are analogous to those obtained at the MP2 level with the same basis set for configurations A and B, while for C they tend to underestimate the interaction energies. Test calculations with the two DFT methods using larger basis sets, 6-311++G$(2d,2p)$ and aug-cc-pVTZ, provide similar results to the ones reported in Table I.

The MP2 results with the aug-cc-pVDZ basis set provide larger interaction energies than those obtained with Pople's basis set, 6-31+G(d,p) and 6-311++G$(2d,p)$. However, the MP2/aug-cc-pVTZ interaction energies are intermediate between those previously mentioned. In fact, some of our recent investigations have shown that the uncorrected MP2/6-311++G$(2d,2p)$ and MP2/aug-cc-pVTZ interaction energies are very similar.[41,42] The CCSD(T)/aug-cc-pVDZ// MP2/aug-cc-pVDZ single point calculations provide similar values to the MP2 ones with the same basis set.

At the MP2 level, the most stable configuration for a given number of monomers is always the C one, where the HB interaction is with the π-cloud. The second more stable configuration depends on the size of the cluster. Thus, smaller clusters prefer a linear configuration (A) while in larger ones, the cyclic configuration through DHBs (B) is more stable. It should be noted that for the same cluster size,

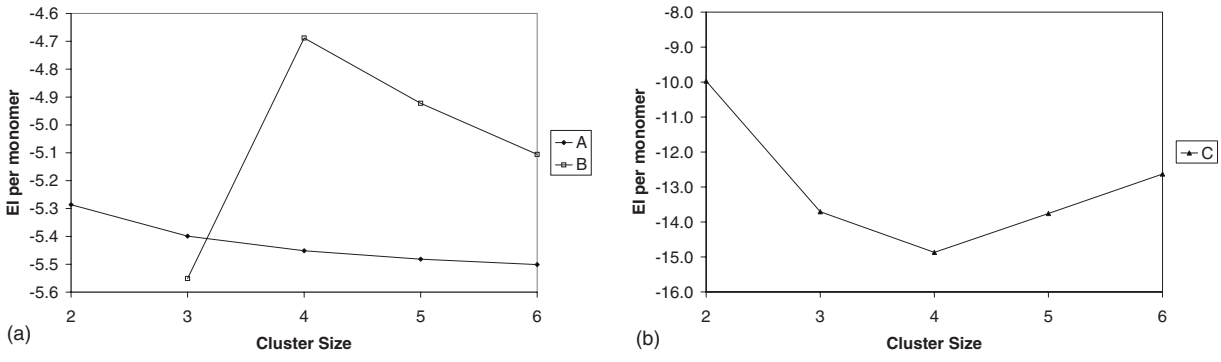

FIG. 3. Interaction energy (kJ/mol) per monomer of the three configurations considered at the MP2/6-31+G(d,p) computational level.

TABLE II. Complexation enthalpies (kJ/mol).

Configuration (No. of monomers)	M05/6-31+G(*d*,*p*)	MP2/6-31+G(*d*,*p*)
A (2)	−4.17	−3.73
A (3)	−8.52	−7.72
A (4)	−12.95	−11.77
A (5)	−17.39	−15.85
A (6)	−21.83	−19.93
B (3)	−12.11	−13.36
B (4)	−12.61	−13.10
B (5)	−17.67	−16.57
B (6)	−22.86	−20.85
C (2)	−5.13	−7.60
C (3)	−15.22	−21.71
C (4)	−23.86	−35.17
C (5)	−29.44	−44.47
C (6)	−36.76	−52.87

the cyclic configurations present one DHB interaction more than those obtained in the linear disposition. In large clusters, the small energetic penalty of the nonlinear DHB is compensated by the larger number of DHBs.

For the discussion of the cooperativity effects, the MP2/6-31+G(*d*,*p*) results will be used as reference since all the methods present similar tendencies. Otherwise, it will be mentioned within the text.

The representation of the interaction energy per monomer at the MP2/6-31+G(*d*,*p*) level is shown in Fig. 3. Configuration A presents a uniform increment in the interaction energy per monomer as the size of the cluster increases, similar to the profile described for the $(HCN)_n$ and $(HNC)_n$ clusters.[19] In configuration B, the strange behavior of the trimer can be explained based on an interaction of the Be atoms with the π-cloud of another molecule, as will be discussed later. Finally, the profile of configuration C indicates that the tetramer is the cluster with the larger interaction energy per monomer since the angle between each pair of interacting molecules is 90°, which is close to the ideal disposition to interact with the π-cloud.

The cooperativity effect considering the average interaction energy of each complex with respect to that observed in the corresponding dimers[43,44] is 4% in the hexamer structure in configuration A and 12% in the tetramer in configuration C, decreasing up to 5% in the hexamer. In the case of the cyclic B structure, no positive cooperativity is observed since the hexamer structure considered is not able to overcome the curvature of the interaction.

The complexation enthalpies of the systems considered have been gathered in Table II. The values obtained are slightly smaller than those listed in Table I for the interaction energy but follow the same tendencies observed for them.

TABLE III. HB distances (Å) of the $(HCCBeH)_n$ clusters in configuration A (for the numbering of the HBs, see Fig. 2).

n	First HB	Second HB	Third HB	Fourth HB	Fifth HB
			B3LYP/6-31+G(*d*,*p*)		
2	2.2259				
3	2.2153	2.2162			
4	2.2138	2.2053	2.2145		
5	2.2135	2.2031	2.2034	2.2142	
6	2.2130	2.2028	2.2015	2.2029	2.2138
			M05/6-31+G(*d*,*p*)		
2	2.1917				
3	2.1847	2.1859			
4	2.1835	2.1777	2.1847		
5	2.1831	2.1763	2.1764	2.1843	
6	2.1832	2.1753	2.1742	2.1754	2.1845
			MP2/6-31+*G*(*d*,*p*)		
2	2.2777				
3	2.2703	2.2701			
4	2.2691	2.2614	2.2690		
5	2.2692	2.2608	2.2604	2.2681	
6	2.2686	2.2596	2.2584	2.2595	2.2686

TABLE IV. HB distances (Å) of the $(HCCBeH)_n$ clusters in configuration B $(HCCBeH)_n$.

n	B3LYP/6-31+G(*d*,*p*)	M05/6-31+G(*d*,*p*)	MP2/6-31+G(*d*,*p*)
3	2.6605	2.5310	2.5443
4	2.4642	2.3812	2.4304
5	2.3567	2.3078	2.3536
6	2.3049	2.2615	2.3152

C. Cluster: Geometry

The interatomic distances of the DHB formed in configurations A and B are reported in Tables III and IV. For configuration C, the distance between the protic hydrogen and the geometrical center of the two carbon atoms that form the triple bond are gathered in Table V. The evolution of the HB distances for configuration A at the MP2/6-31+G(*d*,*p*) level is represented in Fig. 4. It is clear that as the cluster size increases the HB distance in the central HBs becomes shorter. Similar results have been recently reported in a study on the cooperativity effect of H-bonding chains of 4-pyridone.[45] In the case of configuration B (Table IV), it is clear that for larger clusters, the HB distance becomes shorter as an additional proof of cooperativity. Finally, in configuration C (Table V), the shortest distance corresponds to the dimer, as an indication that the cyclic configurations are a compromise between maximizing the number of HBs and the strength of the individual one. As indicated previously, in larger clusters, the smallest distance corresponds to the tetramer, as indicated previously, since it corresponds to the most adequate disposition of the monomers for interaction with the π-cloud.

TABLE V. Distance between the protic hydrogen and the geometrical center of the triple bonds in the clusters with configuration C.

n	B3LYP/6-31+G(*d*,*p*)	M05/6-31+G(*d*,*p*)	MP2/6-31+G(*d*,*p*)
2	2.804	2.714	2.621
3	2.835	2.729	2.653
4	2.749	2.663	2.578
5	2.783	2.683	2.606
6	2.833	2.714	2.647

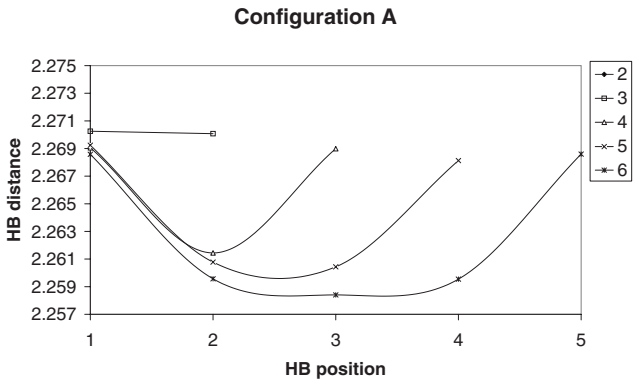

FIG. 4. Evolution of the HB distance along the chains in configuration A for the different clusters studied at the MP2/6-31+G(d,p) computational level.

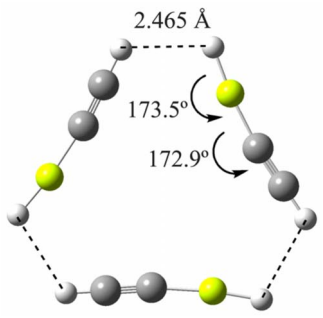

FIG. 5. (Color online) Geometry of the optimized $(HBeCCH)_3$ cluster in configuration B at the MP2/6-311++G(2d,2p) level.

An interesting geometrical feature is the lack of linearity of the $(HBeCCH)_3$ cluster in configuration B, where the HBeC angle became 175.4° and 173.5° at the MP2/6-31+G(d,p) and MP2/6-311++G(2d,2d) levels, respectively, with the Be atoms toward the π-cloud of an adjacent molecules, as can be seen in Fig. 5. In the rest of the clusters of the same configuration, this angle deviates by less than 0.5° from being perfectly linear.

D. Electronic properties

Among the electronic parameters that have been shown to be affected by the cooperativity effect, the dipole moment has been widely used. The values of dipole moment obtained for the clusters in configuration A are reported in Table VI. Due to symmetry, the dipole moments of the clusters in configurations B and C are zero, except for the dimer of configuration C, where the value is 1.56 D. A representation of the dipole moment per monomer (Fig. 6) shows an increment in the average dipole moment enhancement as the cluster size increases, an indication of cooperative effect. Similar results have been reported for the linear $(HCN)_n$ clusters.[19]

The calculated values obtained with the different computational methods show that the dipole moment obtained with the MP2/6-311++G(2d,2p) method are identical to the aug-cc-pVTZ ones and very similar to the M05-2x ones.

Another property that is affected by the cooperativity effect and simultaneously is able to explain it corresponds to the values of the electrostatic potential in the regions where the interaction occurs. In one hand, it shows deeper minima as the number of monomers increases in the linear disposition (Table VII). These effects indicate that these centers will form stronger interactions when a new monomer approaches those clusters. The values obtained with the M05 and MP2 computational levels, even though different, present a perfectly linear relationship.

The analysis of the orbital interaction between the interacting molecules shows two different patterns. In the clusters formed by DHB, the main intermolecular orbital interaction corresponds to the charge transfer between the occupied BeH σ bond with the empty σ^* C–H one. In the complexes in configuration C, the charge transfer observed is between the π orbital of the CC bond and the empty σ^* CH one. The values of those interactions have been gathered in Table VIII. It is significant that the sum of all these interactions for a given cluster provides a value very similar to that obtained in the interaction energy. In addition, the larger orbital interactions are between the monomers that are located approximately in the middle of the chain, in good agreement with the observed shorter distances obtained for these interactions (Table II).

The charge transfer between orbitals of different molecules justifies the increment in the dipole moment observed in the cluster. At the same time, this effect produces an increment in charge ($\delta-$) in the monomer located at the end of the chain that will act as HB acceptor and a deficiency ($\delta+$) in the other extreme of the chain. These effects are qualitatively able to explain the cooperativity observed in the chains in A disposition and are analogous to that observed in other HB clusters.[34,43]

E. AIM

The topological analysis of the electron density shows the presence of new bond critical points (bcps) due to the new interactions formed (Fig. 7). In all the cases, the values of the electron density are small (between 5×10^{-3} and 6×10^{-3} in the DHB and between 8×10^{-3} and 9×10^{-3} in

TABLE VI. Dipole moments (D) of the $(HBeCCH)_n$ clusters in configuration A.

n	B3LYP/6-31+G(d,p)	M05/6-31+G(d,p)	MP2/6-31+G(d,p)	MP2/6-311++G(2d,2p)	MP2/aug-cc-pVDZ	MP2/aug-cc-pVTZ
1	1.01	0.92	0.94	0.92	0.95	0.92
2	2.53	2.20	2.30	2.29	2.38	2.29
3	4.11	3.58	3.70	3.69	3.86	
4	5.69	4.99	5.11	5.06	5.36	
5	7.28	6.39	6.53	6.51		
6	8.87	7.81	7.95			

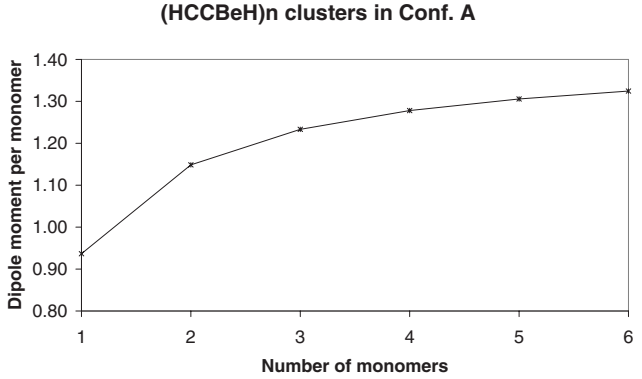

FIG. 6. Average dipole moment (D) per monomer of the cluster in configuration A calculated at the MP2/6-31+G(d,p) computational level.

the π-HB) and the values of the Laplacian are small and positive (0.017–0.019 in the DHB and 0.023–0.025 in the π-HB).

The integration within the atomic basins provides a tool to analyze the charge and energy flow due to the molecular interactions. The values obtained for the atomic charge, energy, and volume in the isolated monomer obtained at the MP2/6-31+G(d,p) level are represented in Fig. 8 and will be used as reference to compare the results obtained in the complexes.

The charge analysis within the linear complexes (configuration A) shows in the monomers at both ends a charge of 8 me, negative for the monomer that interacts with the protic hydrogen and positive for the monomer that interacts with the hydric one. All the intermediate monomers are approximately neutral. A more detailed analysis shows that C(3) became more negatively charged (25 me in average) in all the monomers that were isolated while the C(2)–H(1) atoms lost charge (9 and 15 me, respectively).

Regarding, the energetic variations, the first monomers lost energy, while most of the gain concentrated in the central monomers probably due to the formation of two DHBs. At an atomic level, the energy gains are concentrated in the C(3) and H(5) (37 and 5 kJ/mol, respectively) and the losses in the C(2), H(1), and Be(4) atoms (10, 19, and 8 kJ/mol, respectively).

With respect to the volume, the variations observed are small, the cluster volume being slightly larger than the sum of the isolated monomers in the dimer and trimer, no variation in the tetramer, and smaller than five isolated monomers in the pentamer. Probably, the cooperative effect is able to compress the cluster to observe a decrease for clusters larger than that for the tetramer. Along the chain, a loss of volume is observed in the first monomer and gain in the last, with minimum variations in the rest.

TABLE VII. Values of the minimum electrostatic potential (a.u.) along the symmetry axis for the $(HBeCCH)_n$ clusters in configuration A.

n	M05/6-31+G(d,p)	MP2/6-31+G(d,p)
1	−0.0153	−0.0199
2	−0.0178	−0.0224
3	−0.0185	−0.0230
4	−0.0187	−0.0233
5	−0.0189	−0.0235
6	−0.0190	−0.0236

TABLE VIII. Orbital interaction energies (kJ/mol) obtained with the NBO method at the M05/6-31+G(d,p) computational level.

n	A[a]	B[b]	C[b]
2	4.9		6.6
3	5.1, 5.1	0.8	6.1
4	5.2, 5.3, 5.1	3.1	8.2
5	5.2, 5.4, 5.4, 5.1	4.2	7.6
6	5.2, 5.4, 5.4, 5.5, 5.1	4.9	6.4

[a]Listed in the same order as in Fig. 2
[b]Value for each individual intermolecular orbital interaction.

In the complexes in configuration B, due to symmetry the charge variation is null and the energy gain due to the complex formation is uniformly distributed in all the monomers. At an atomic level, the same tendencies discussed for the complexes in configuration A are observed.

In the dimers of configuration C, all the atoms of the HB donor monomer lose charge that goes mainly to the C(3) of the acceptor monomer. Something similar is observed in the energy, where the C(3) of the acceptor monomer gains 47 kJ/mol due to the loss of the H(1) of the donor and acceptor monomers (10 and 22 kJ/mol, respectively).

In the cyclic clusters of configuration C, the redistribution of the charge of the monomers produces an electronic loss in H(1) and C(2) (in average 27 and 8 me, respectively) and a gain in C(3) (40 me in average).

F. CH stretching frequencies

Among the variation observed in the formation of a HB complex, the variation in the XH bond stretching in the HB donor has been used for a long time, characteristic of the existence of a complex. In general, a redshift is observed but recently some cases with blueshifts have been described. The CH frequencies obtained for the clusters studied here have been gathered in Table IX. In agreement with previous find-

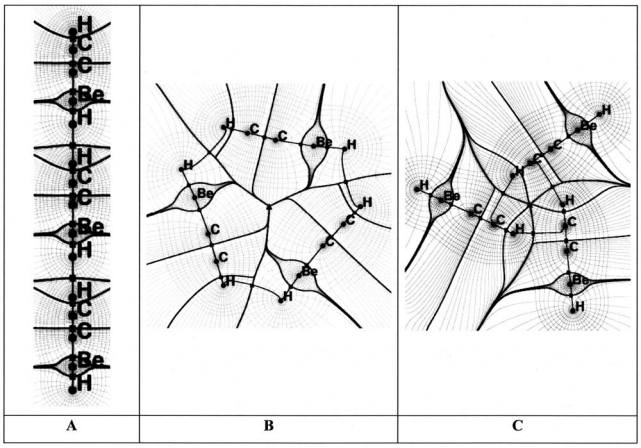

FIG. 7. Electron density maps of the cyclic trimer of HCCBeH calculated at the MP2/6-31+G(d,p) computational level. The atoms, bcps, and ring critical points are indicated by dots, squares, and triangles, respectively. The atomic interatomic surfaces are shown.

	Charge	Energy	Volume
H(1)	0.1319	-0.56481	43.0
C(2)	-0.5258	-38.19990	140.7
C(3)	-0.4743	-37.94665	167.4
Be(4)	1.7224	-14.27375	17.9
H(5)	-0.8542	-0.79024	138.0

FIG. 8. Atomic values (a.u.) of the isolated monomer calculated at the MP2/6-31+G(d,p) level within the AIM methodology.

ings, the larger variations in the CH stretching correspond to the clusters in the C configuration, which are the ones showing the stronger interaction energies. With respect to the DHB clusters, the larger variations in the clusters in the A configuration correspond to the central CH moieties, and in the clusters in the B configuration, the variation tends asymptotically toward a limit value as the size of the cluster increases.

The values of the CH stretching are highly correlated with the corresponding bond length and with the orbital interactions calculated with the NBO methods (Fig. 9). Thus, this parameter can be used to estimate the value of the geometrical parameter and the strength of the individual interaction.

IV. CONCLUSIONS

A theoretical study of three possible arrangements of the $(HCCBeH)_n$ clusters has been carried out using DFT and *ab initio* MP2 methods. The analysis of the results show that the most stable conformation corresponds to that where the interaction occurs between the proton hydrogen of one molecule and the π-cloud of another. Cooperative effects are observed in those configurations where DHBs are the main force holding together the clusters. Thus, a shortening of the DHB distance and an increment in the interaction energy and dipole moment per monomer are observed.

The intermolecular orbital interaction, calculated within the NBO methodology, is able to explain the source of the interaction between the monomers. This parameter shows that the interactions in the center of the chain are stronger than those found in the extreme of the chain.

TABLE IX. CH bond stretching (cm^{-1}) calculated at the MP2/6-31+G(d,p) computational level.

	A							
n	Free	HB1	HB2	HB3	HB4	HB5	B	C
1	3500.6							
2	3501.1	3486.2						3478.0
3	3500.7	3484.2	3484.7				3499.9	3470.4
4	3500.7	3484.2	3482.9	3484.3			3491.0	3464.7
5	3500.7	3484.2	3483.0	3482.5	3484.2		3485.3	3467.5
6	3500.7	3484.1	3482.9	3482.2	3482.7	3484.2	3484.1	3473.1

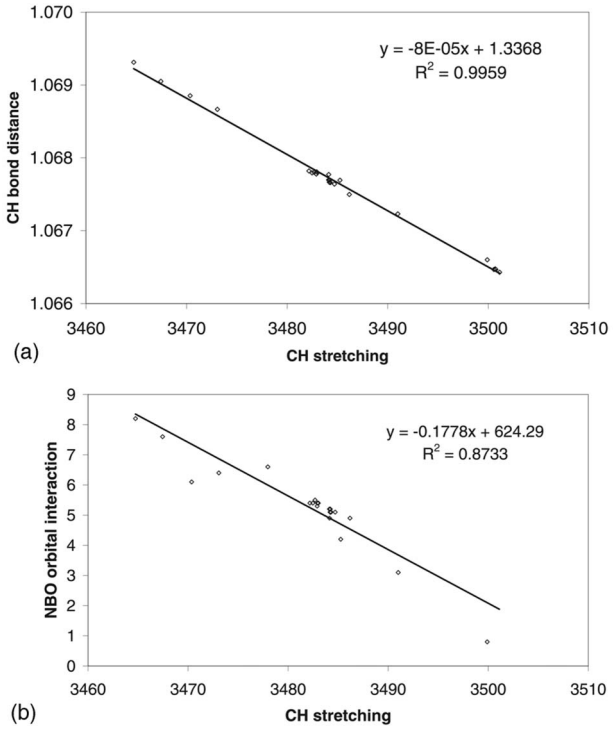

FIG. 9. CH stretching (cm^{-1}) vs the CH bond distance and σ(BeH) $\rightarrow \sigma^*$(CH) orbital interaction.

The deeper minima of the MEP values as the size of the chain increases explain the cooperativity effect observed.

ACKNOWLEDGMENTS

M. Solimannejad acknowledges the travel grant provided by CSIC and Arak University. This work was carried out with financial support from the Ministerio de Ciencia y Tecnología (Grant Nos. CTQ2006-14487-C02-01/BQU and CTQ2007-61901/BQU) and Comunidad Autónoma de Madrid (Project MADRISOLAR, Reference No. S-0505 /PPQ/0225). Thanks are given to CESGA and CTI (CSIC) for allocation of computer time.

[1] O. Mó, M. Yáñez, and J. Elguero, J. Chem. Phys. **97**, 6628 (1992).
[2] M. Mohr, D. Marx, M. Parrinello, and H. Zipse, Chem.-Eur. J. **6**, 4009 (2000).
[3] M. Mohr and H. Zipse, Phys. Chem. Chem. Phys. **3**, 1246 (2001).
[4] S. Scheiner, *Hydrogen Bonding: A Theoretical Perspective* (Oxford University Press, Oxford, 1997).
[5] M. P. Brown and R. W. Heseltin, Chem. Commun. **1968**, 1551.
[6] R. H. Crabtree, P. E. M. Siegbahn, O. Eisenstein, and A. L. Rheingold, Acc. Chem. Res. **29**, 348 (1996).
[7] R. Custelcean and J. E. Jackson, Chem. Rev. **101**, 1963 (2001).
[8] I. Alkorta, I. Rozas, and J. Elguero, Chem. Soc. Rev. **27**, 163 (1998).
[9] V. I. Bakhmutov, *Dihydrogen Bonds: Principles, Experiments and Applications* (Wiley, Hoboken, NJ, 2008).
[10] P. L. A. Popelier, J. Phys. Chem. A **102**, 1873 (1998).
[11] S. Grabowski, W. A. Sokalski, and J. Leszczynski, J. Phys. Chem. A **108**, 5823 (2004).
[12] S. J. Grabowski, W. A. Sokalski, and J. Leszczynski, Chem. Phys. **337**, 68 (2007).
[13] I. Alkorta, J. Elguero, and C. Foces Foces, Chem. Commun. **1996**, 1633.
[14] I. Alkorta, K. Zborowski, J. Elguero, and M. Solimannejad, J. Phys. Chem. A **110**, 10279 (2006).
[15] J. G. Planas, C. Viñas, F. Teixidor, A. Comas-Vives, G. Ujaque, A. Lledós, M. E. Light, and M. B. Hursthouse, J. Am. Chem. Soc. **127**, 15976 (2005).

[16] N. V. Belkova, T. N. Gribanova, E. I. Gutsul, R. M. Minyaev, C. Bianchini, M. Peruzzini, F. Zanobini, E. S. Shubina, and L. M. Epstein, J. Mol. Struct. **844–845**, 115 (2007).
[17] K. Nauta and R. E. Miller, Science **283**, 1895 (1999).
[18] P. F. Provasi, G. A. Aucar, M. Sanchez, I. Alkorta, J. Elguero, and S. P. A. Sauer, J. Phys. Chem. A **109**, 6555 (2005).
[19] M. Sanchez, P. F. Provasi, G. A. Aucar, I. Alkorta, and J. Elguero, J. Phys. Chem. B **109**, 18189 (2005).
[20] G. A. Jeffrey and W. Saenger, *Hydrogen Bonding in Biological Structures* (Springer-Verlag, Berlin, 1991).
[21] C. A. Thompson and L. Andrews, J. Am. Chem. Soc. **118**, 10242 (1996).
[22] M. J. Frisch, G. W. Trucks, and H. B. Schlegel *et al.*, GAUSSIAN 03, Gaussian, Inc., Wallingford, CT, 2003.
[23] A. D. Becke, J. Chem. Phys. **98**, 5648 (1993).
[24] C. T. Lee, W. T. Yang, and R. G. Parr, Phys. Rev. B **37**, 785 (1988).
[25] P. C. Hariharan and J. A. Pople, Theor. Chim. Acta **28**, 213 (1973).
[26] Y. Zhao, N. E. Schultz, and D. G. Truhlar, J. Chem. Theory Comput. **2**, 364 (2006).
[27] C. Møller and M. S. Plesset, Phys. Rev. **46**, 618 (1934).
[28] M. J. Frisch, J. A. Pople, and J. S. Binkley, J. Chem. Phys. **80**, 3265 (1984).
[29] T. H. Dunning, J. Chem. Phys. **90**, 1007 (1989).
[30] S. F. Boys and F. Bernardi, Mol. Phys. **19**, 553 (1970).
[31] D. W. Schwenke and D. G. Truhlar, J. Chem. Phys. **82**, 2418 (1985).
[32] D. B. Cook, J. A. Sordo, and T. L. Sordo, Int. J. Quantum Chem. **48**, 375 (1993).
[33] M. J. Frisch, J. E. Del Bene, J. S. Binkley, and H. F. Schaefer III, J. Chem. Phys. **84**, 2279 (1986).
[34] B. F. King and F. Weinhold, J. Chem. Phys. **103**, 333 (1995).
[35] R. F. W. Bader, *Atoms in Molecules: A Quantum Theory* (Clarendon, Oxford, 1990).
[36] F. W. Biegler-König, R. F. W. Bader, and T. H. Tang, J. Comput. Chem. **3**, 317 (1982).
[37] P. L. A. Popelier, with a contribution from R.G.A. Bone (UMIST, England, EU) MORPHY 98, a topological analysis program, 1999.
[38] F. W. Biegler-König and J. Schönbom, AIM2000, Bielefeld, Germany, 2002.
[39] I. Alkorta and O. Picazo, ARKIVOC IX, 305 (2005).
[40] A. E. Reed, L. A. Curtiss, and F. Weinhold, Chem. Rev. **88**, 899 (1988).
[41] M. Solimannejad, I. Alkorta, and J. Elguero, Chem. Phys. Lett. **449**, 23 (2007).
[42] I. Alkorta, F. Blanco, and J. Elguero, J. Phys. Chem. A **112**, 6753 (2008).
[43] R. D. Parra, S. Bulusu, and X. C. Zeng, J. Chem. Phys. **122**, 184325 (2005).
[44] H. Guo and M. Karplus, J. Phys. Chem. **98**, 7104 (1994).
[45] Y. F. Chen and J. J. Dannenberg, J. Am. Chem. Soc. **128**, 8100 (2006).